Title: Sulforaphane induces lipophagy through the activation of AMPK-mTOR-ULK1 pathway signaling in adipocytes

Authors: Masashi Masuda[a,*,†], Risa Yoshida-Shimizu[a,†], Yuki Mori[a,†], Kohta Ohnishi[a,l], Yuichiro Adachi[a], Maiko Sakai[a], Serina Kabutoya[a], Hirokazu Ohminami[a], Hisami Yamanaka-Okumura[a], Hironori Yamamoto[a,b,c], Makoto Miyazaki[d], Yutaka Taketani[a]

Affiliations: [a]Department of Clinical Nutrition and Food Management, Institute of Biomedical Sciences, Tokushima University Graduate School, Tokushma, Tokushima 770-8503, Japan. [b]Department of Health and Nutrition, Faculty of Human Life, Jin-ai University, Echizen, Fukui 915-8586, Japan, [c]Department of Nephrology, Faculty of Medical Sciences, University of Fukui, Fukui 910-1193, Japan. [d]Division of Renal Diseases and Hypertension, Department of Medicine, University of Colorado Denver, Aurora, Colorado 80045, USA.

[†]These authors contributed equally to this work.

*To whom correspondence should be addressed: Masashi Masuda, Ph. D.

Department of Clinical Nutrition and Food Management, Institute of Biomedical Sciences, Tokushima University Graduate School, Tokushma, Tokushima, Japan

3-18-15, Kuramoto-cho, Tokushima 770-8503, Japan

Phone: +81-88-633-7235

E-mail: masuda.masashi@tokushima-u.ac.jp

†Contributed equally to this work.

[1] **Present address:** Laboratory of Animal Science, Graduate School of Life and Environmental Sciences, Kyoto Prefectural University, Kyoto 606-8522, Japan

Funding sources: This work was supported by JSPS KAKENHI Grant Numbers JP17K19910, JP20K21761 (to M. Masuda), JP16H03046, JP19H04053 (to Y. Taketani), and Uehara Memorial Foundation (to M. Masuda).

Abstract

Lipophagy, a form of selective autophagy, degrades lipid droplet (LD) in adipose tissue and the liver. The chemotherapeutic isothiocyanate sulforaphane (SFN) contributes to lipolysis through the activation of hormone-sensitive lipase and the browning of white adipocytes. However, the details concerning the regulation of lipolysis in adipocytes by SFN-mediated autophagy remain unclear. In this study, we investigated the effects of SFN on autophagy in the epididymal fat of mice fed a high-fat diet (HFD) or control-fat diet (CFD) and on the molecular mechanisms of autophagy in differentiated 3T3-L1 cells. Western blotting revealed that the protein expression of lipidated LC3 (LC3-II), an autophagic substrate, was induced after 3T3-L1 adipocytes treatment with SFN. In addition, SFN increased the LC3-II protein expression in the epididymal fat of mice fed an HFD. Immunofluorescence showed that the SFN-induced LC3 expression was co-localized with LDs in 3T3-L1 adipocytes and with perilipin, the most abundant adipocyte-specific protein, in adipocytes of mice fed an HFD. Next, we confirmed that SFN activates autophagy flux in differentiated 3T3-L1 cells using the mCherry-EGFP-LC3 and GFP-LC3-RFP-LC3ΔG probe. Furthermore, we examined the induction mechanisms of autophagy by SFN in 3T3-L1 adipocytes using western blotting. *ATG5* knockdown partially blocked the SFN-induced release of fatty acids from LDs in mature 3T3-L1 adipocytes. SFN time-dependently elicited the phosphorylation of AMPK, the dephosphorylation of mTOR, and the phosphorylation of ULK1 in differentiated 3T3-L1 cells. Taken together, these results suggest that SFN may provoke lipophagy through AMPK-mTOR-ULK1 pathway signaling, resulting in partial lipolysis of adipocytes. (246/250 words)

Keywords: adipose, obesity, autophagy, cell biology, Lipid droplets, dietary factors

Introduction

Obesity, a major public health problem, causes or exacerbates many other health problems and diseases, such as diabetes mellitus, coronary heart disease, and certain forms of cancer [1]. Obesity is caused by an imbalance between energy intake and expenditure that results in adipose tissue dysfunction with adipocyte hypertrophy [2]. Four mechanisms have been proposed for treating obesity: stimulating thermogenesis, suppressing appetite, lowering adipogenesis, and enhancing lipolysis [3]. Certain dietary factors, such as phosphate, caffeine, and sulforaphane (SFN), can regulate lipolysis in adipose tissue [4−7].

Lipolysis has long been recognized as a biochemical catabolic pathway that relies on the direct activation of lipid droplet (LD)-associated lipases, such as adipose triglyceride lipase (ATGL), hormone-sensitive lipase (HSL), and monoglyceride lipase [8]. Surprisingly, a major discovery in the field of lipolysis in hepatocytes was the realization that autophagy, an intracellular catabolic pathway, is also used to deliver LDs as cargo to lysosomes for hydrolysis, in a process known as lipophagy [9]. Autophagy is one of the major degradation pathways in cells supporting the survival of cells by recycling metabolic components. Autophagy can be induced in cells through the activation of the stress-sensing kinase AMPK or the inhibition of the nutrient-sensing kinase mTORC1 [10, 11]. The phosphorylation of AMPK and the inhibition of mTORC1 can activate the serine/threonine kinase ULK complex, which drives the formation of a phagophore, the initial autophagosomal precursor membrane structure [11, 12]. During autophagy, LC3 is conjugated to the phosphatidylethanolamine (PE) molecule on the isolation membrane as lipidated LC3 (LC3-II), an autophagy substrate, by the ATG12-

ATG5-ATG16 complex after cleavage of glycine 120 residues of LC3 by ATG4 [13−18]. Interestingly, it has been suggested that lipophagy may contribute to lipolysis in adipocytes, including *in vitro* and *in vivo* [19−22]. Lipophagy is caused by aging and nutrient starvation; however, the effects of dietary factors on lipophagy in adipocytes remain unclear.

The chemotherapeutic isothiocyanate SFN is a natural compound obtained from broccoli sprouts. SFN is the major inducer of phase II detoxifying enzymes through the Kelch-like ECH-associated protein 1 (Keap1)/nuclear factor E2-related factor 2 (Nrf2)/antioxidant response element (ARE) signaling pathway [23−25]. Keap1 functions as a chemical sensor of cellular redox tone, mediating the activation of Nrf2 [26]. Under basal conditions, Keap1 sequesters Nrf2 within a complex with Cullin3, which is an E3 ubiquitin ligase that targets Nrf2 for proteasomal degradation [27]. Nrf2 activated by SFN interacts with Keap1, leading to the dissociation or degradation of the Cullin3-Keap1 complex and stabilization of Nrf2, which translocates to the nucleus, thereby activating ARE-dependent genes [28]. Nrf2-Keap1 is closely related to the autophagy pathway through p62, also called sequestosome 1, which acts as a cargo receptor for autophagic degradation of ubiquitinated targets [29, 30]. Nrf2 activation induces p62 which competitively inhibits the Keap1-Nrf2 interaction and binds to the Keap1, resulting in the induction of autophagy [30−32]. Interestingly, LC3 promotes the movement of cytoplasmic ATGL to LDs through interaction with the LC3-interacting region (LIR) domain of ATGL and induces lipophagy [33]. Lipase and lipophagy are suggested to exhibit complementarity and cooperativity toward total lipolysis. SFN may contribute to lipolysis through the activation of HSL and the browning of white adipocytes [7, 34]. However, the

1 regulation of lipolysis by SFN in adipocytes focused on lipophagy, but not lipase and adipocyte browning, has not
2 yet been identified.
3 In the present study, we examined the possible contribution of SFN to lipolysis through lipophagy in
4 adipocytes from mice fed a high-fat diet (HFD) or control-fat diet (CFD) and *in vitro* in mature 3T3-L1
5 adipocytes. We also investigated the mechanisms underlying lipophagy induction by SFN in differentiated 3T3-
6 L1 cells.
7
8

Materials and Methods

Chemicals and reagents

DMSO, mouse anti-β-actin monoclonal Ab (A5441), 4',6-diamidino-2-phenylindole (DAPI; D9542), DMEM, FBS, insulin, dexamethasone, 3-isobutyl-1-methylxanthine, and troglitazone were purchased from Sigma-Aldrich (St. Louis, MO, USA). D, L-Sulforaphane was purchased from Toronto Research Chemicals (Toronto, Canada). Buprenorphine hydrochloride was purchased from Otsuka Pharmaceutical Co., Ltd. (Tokyo, Japan). Pentobarbital sodium salt was purchased from Tokyo Kasei Co., Ltd. (Tokyo, Japan). RIPA buffer, anti-Perilipin-1 (#9349), anti-LC3 (#2775), anti-p62 (#5114), anti-AMPKα (#5831), anti-phospho-AMPKα (#50081, Thr172), anti-mTOR (#2972), anti-phospho-mTOR (#2971, Ser2448), anti-ULK1 (#8054), anti-phospho-ULK1 (#5869, Ser555), anti-4E-BP1 (#8594), anti-phospho-4E-BP1 (#9451, Ser65), anti-Histone H3 (#5192), anti-p44/42 MAPK (Erk1/2; #9102), anti-phospho-p44/42 MAPK (Erk1/2; #4377), and anti-Rubicon (#8465) Ab were purchased from Cell Signaling Technology (Beverly, MA, USA). Anti-MAP LC3β (sc-271625), anti-Nrf2 (sc-365945), anti-Keap1 (sc-15246), and anti-SIRT1 (sc-74465) Ab were purchased from Santa Cruz Biotechnology (Santa Cruz, CA, USA). Goat anti-rabbit IgG(H+L)-HRP conjugate (#1706515) was purchased from Bio-Rad (Hercules, CA, USA). Goat anti-mouse IgG(H+L)-HRP conjugate (#62-6520), Alexa Fluor® 488, Alexa Fluor® 555, Alexa Fluor® 568, ProLong™ Diamond Antifade Mountant (P36965), and BODIPY 493/503 (D3922) were purchased from Invitrogen (Carlsbad, CA, USA). ECL Plus system and poly(dI-dC) were purchased from GE Healthcare (Buckinghamshire, UK). OCT compound was purchased from Sakura FineTek (Tokyo, Japan). Calf serum was purchased from Hyclone

(Logan, UT, USA). Penicillin-streptomycin was purchased from Nacalai Tesque (Kyoto, Japan). FuGENE® HD Transfection Reagent was purchased from Promega Corporation (Madison, WI, USA). Bafilomycin A1 (Bafilomycin) was purchased from Enzo Life Sciences (Ann Arbor, MI, USA). FluoroBrite™ DMEM (A1896701), Lipofectamine RNAiMAX transfection reagent, TRIzol™ Reagent, oligo(dT) primer, and SYBR® Green master mix were purchased from Thermo Fisher Scientific (Waltham, MA, USA). M-MLV reverse transcriptase was purchased from Nippon Gene (Tokyo, Japan).

Cell culture and establishment of stable cell lines

Mouse fibroblast line 3T3-L1 pre-adipocytes (JCRB9014) were obtained from the Health Science Research Resources Bank (Osaka, Japan). The 3T3-L1 pre-adipocytes were cultured as described previously [5]. Briefly, 3T3-L1 pre-adipocytes were maintained in high-glucose DMEM containing 10% calf serum and 1% penicillin-streptomycin at 37˚C in an atmosphere containing 5% CO_2. To induce the differentiation of the pre-adipocytes into mature adipocytes, 100% confluent cells were maintained for 2 days and changed to differentiation medium (DMEM containing 10% FBS, 10 μg/ml insulin, 1 μM dexamethasone, 500 μM 3-isobutyl-1-methylxanthine, and 1 μM troglitazone). Two days later, the media were replaced with DMEM containing 10% FBS and refreshed every other day for an additional 6 days.

Retroviral plasmid vector of pBABE-puro mCherry-EGFP-LC3 (#22418) developed by Dr. Jayante Debnath was obtained from Addgene (Cambridge, MA, USA) [35]. Retroviral plasmid vector of pMRX-IP-GFP-LC3-RFP-

LC3ΔG (RDB14600) developed by Dr. Noboru Mizushima was obtained from RIKEN BRC DNA BANK (Tsukuba, Japan) [36]. These plasmids were respectively transfected into 90% confluent 3T3-L1 cells using FuGene® HD Transfection Reagent for 48 h. The medium was replaced with a medium containing the final concentration of 2 μg/ml puromycin for 10 days. Fluorescence of 3T3-L1 cells colony was observed by an EVOS FLoid Cell Imaging Station (Thermo Fisher Scientific) and bright colonies were transferred to new a dish for the experiments.

Cell viability assay

To determine the effect of SFN on the cell survival in 3T3-L1 cells, cells were differentiated into mature adipocyte and treated with vehicle (DMSO) or SFN (10 and 100 μM) for 10 days. Cell survival was tested using a CellTiter-Fluor™ Cell Viability Assay (Promega, Madison, WI, USA) according to the manufacture's instruction The CellTiter-Fluor™ reagent was added to wells, and viability was measured after incubation at 37˚C for 120 min. The fluorescence spectra were measured using SpectraMax i3 (Molecular Devices, Sunnyvale, CA, USA) with filter set at Ex/Em 390/505 nm.

Oil Red-O staining

To determine the triglycerides accumulated in 3T3-L1 cells, oil red-O staining was performed using 24-well tissue culture plates. Cells were differentiated into mature adipocyte, followed by the treatment with vehicle (DMSO), SFN (10 and 100 μM), or 500 nM rapamycin for 10 days. After removing the medium and washing twice with PBS,

the cells were fixed with 4% PFA/PBS for 10 min. After washing with PBS, 60% isopropanol was added for 1 min and stained with oil red-O diluted with 60% isopropanol for 20 min. After rinsing with 60% isopropanol and PBS, the cells were photographed under a BZ-9000 fluorescence microscope (Keyence, Osaka, Japan). Lipid accumulation was quantified using the ImageJ imaging software program (NIH, Bethesda, MD, USA).

Western blot analysis

Nuclear extracts from mammalian cells were prepared as described previously [37]. Tissue and cell lysates were prepared using RIPA buffer. Protein samples were heated at 95˚C for 5 min in sample buffer in the presence of 5% 2-mercaptoethanol and subjected to SDS-PAGE. The separated proteins were transferred by electrophoresis to polyvinylidene difluoride transfer membranes (Immobilon-P, Millipore, MA, USA). The membranes were treated with diluted affinity-purified anti-LC3 (1:3000), anti-p62 (1:3000), anti-AMPKα (1:3000), anti-phospho-AMPKα (1:1500), anti-mTOR (1:3000), anti-phospho-mTOR (1:1500), anti-ULK1 (1:3000), anti-phospho-ULK1 (1:1500), anti-4E-BP1 (1:3000), anti-phospho-4E-BP1 (1:1500), anti-p44/42 MAPK (1:3000), anti-phospho-p44/42 MAPK (1:3000), anti-Rubicon (1:3000), anti-Nrf2 (1:3000), anti-Keap1 (1:3000), and anti-SIRT1 (1:3000) Ab. Mouse anti-β-actin monoclonal Ab and anti-Histone H3 Ab were used as an internal control. Goat anti-rabbit IgG(H+L)-HRP conjugate and goat anti-mouse IgG(H+L)-HRP conjugate were utilized as a secondary Ab, and signals were detected using the ECL Plus system.

Immunocytochemical analysis

Differentiated 3T3-L1 cells on glass coverslips were treated with vehicle (DMSO) or 10 μM SFN for 3 h, fixed with 4% PFA/PBS at RT for 15 min, washed 2 times in PBS, and processed for immunofluorescence by permeabilization with 0.1% Triton X-100/PBS for 5 min on ice. After washing with PBS, the blocking was carried out by 0.8% BSA/PBS at RT for 30 min. The cells were incubated with anti- LC3 (1:200) for 1 h, after which they were washed and labeled with Alexa Fluor 568 (1:200). To detect LDs, BODIPY 493/503 was diluted in PBS at a concentration of 6.25 μM and applied to cells for 30 min. After washing with 0.4% BSA/PBS, sections were mounted in ProLong™ Diamond Antifade Mountant. Fluorescence was visualized using a BZ-9000 fluorescence microscope or a Leica Confocal Microscope (TCS-SL) (Leica Microsystems GmbH, Mannheim, Germany). Quantification of data was performed using the ImageJ imaging software program.

Animal experiments

The animal work took place in Division for Animal Researches and Genetic Engineering Support Center for Advanced Medical Sciences, Institute of Biomedical Sciences, Tokushima University Graduate School. The animals were housed in pathogen-free conditions and maintained under a standard 12 h light-dark cycle with free access to water. Seven-week-old male C57BL/6J mice (Japan SLC, Shizuoka, Japan) were fed HFD, contained 45% kcal as fat, 35% kcal as carbohydrate, 20% kcal as protein with an energy density of 4.73 kcal/gm (No. D12451; Research Diets, New Brunswick, NJ, USA) or control-fat diet (CFD), contained 10% kcal as fat, 70% kcal as carbohydrate,

20% kcal as protein with an energy density of 3.85 kcal/gm (No. D12450H; Research Diets, New Brunswick, NJ, USA) for 8 weeks. After fasting for 18 h, these mice were randomly divided into two groups (n = 4 per group) and intraperitoneally administrated a total of 30 mg/kg body weight of SFN or DMSO prepared in 500 μl sterile saline. Each group of mice was fasted for 3 h with water *ad libitum* before sacrifice with a total of 0.1 mg/kg body weight of buprenorphine hydrochloride and a total of 50 mg/kg body weight of pentobarbital sodium salt. Epididymal fat samples were washed in 0.9% NaCl and immediately snap-frozen in liquid nitrogen and stored at −80˚C. The present study was approved by the Animal Experimentation Committee of Tokushima University School of Medicine (animal ethical clearance No. T28-88) and was carried out in accordance with guidelines for the Animal Care and Use Committee of Tokushima University School of Medicine.

Plasma parameters

Plasma triglyceride (TG) and non-esterified fatty acid (NEFA) levels were determined using commercial kit LabAssay™ Triglyceride (Wako, Osaka, Japan) and LabAssay™ NEFA (Wako) according to the manufacture's instruction, respectively [4]. Absorbance was measured by SpectraMax ABS (Molecular Devices).

Immunofluorescent staining

Epididymal adipose tissues were fixed in cold 4% PFA/PBS for 6 h followed by overnight incubation in 30% sucrose/PBS. The tissues were embedded in OCT compound diluted with 30% sucrose/PBS. Tissues were cryo-

sectioned at 10 μm thickness, air-dried, re-fixed in 4% PFA/PBS for 15 min at room temperature (RT), washed 3 times in PBS, and processed for immunofluorescence by permeabilization with 0.1% Triton X-100/PBS for 5 min, followed by washing 3 times with PBS. Mouse primary antibodies/markers were added to Ab dilution buffer at 37˚C for 2 h: MAP LC3β (1:200) and Perilipin-1 (1:200). After washing with PBS, tissues were incubated for 30 min at RT with secondary antibodies prepared at 1:200 in Ab dilution buffer: Alexa Fluor 488 and Alexa Fluor 555. After the secondary antibodies were removed and tissues were washed with PBS, nuclear counterstaining was performed by incubation with DAPI solution (0.2 μg/ml) at RT for 1 h. After washing with PBS, sections were mounted in ProLong™ Diamond Antifade Mountant. Fluorescence was visualized using a BZ-9000 fluorescence microscope.

Autophagy flux assay

Stable 3T3-L1 cells expressing mCherry-EGFP-LC3 were seeded on glass coverslips. After the differentiation of the pre-adipocytes into mature adipocytes, they were treated with vehicle (DMSO) or 10 μM SFN for 3 h and fixed with 4% PFA/PBS at RT for 15 min. After washing with PBS, cells were incubated with 50 mM NH_4Cl/PBS for 10 min at RT. After washing with PBS, sections were mounted in ProLong™ Diamond Antifade Mountant. Fluorescence was visualized using a BZ-9000 fluorescence microscope.

For GFP-LC3-RFP-LC3ΔG microplate assay, wild-type (as background) or stable 3T3-L1 cells expressing GFP-LC3-RFP-LC3ΔG were seeded into 96-well plates (Greiner CELLSTAR #655090, Greiner Bio-One,

Germany). After the differentiation of the pre-adipocytes into mature adipocytes, they were treated with vehicle (DMSO) or 10 μM SFN for 3 h. Following washing with FluoroBrite™ DMEM twice, cells were imaged by using Operetta high-content imaging system (PerkinElmer, MA, USA) at 40x magnification at following settings: for EGFP (λ ex: 460−490 nm, λ ex: 500−550 nm) and for RFP (λ ex: 530−560 nm, λ ex: 570−650 nm).

RNAi experiments

Differentiated 3T3-L1 cells were transfected with siRNA directed against *ATG5* (SASI_Mm01_00089196 and SASI_Mm01_00089197; Sigma-Aldrich) and negative control (SIC001; Sigma-Aldrich) or against AMPKα1/2 (sc-45313; Santa Cruz Biotechnology) and negative control (sc-37007; Santa Cruz Biotechnology) using Lipofectamine RNAiMAX transfection reagent, according to the manufacture's instruction. The expression levels were assessed after 48 h by quantitative PCR analysis.

Quantitaitve PCR analysis

Total RNA was isolated from 3T3-L1 cells using TRIzol™ Reagent according to the manufacture's instruction. Quantitative real-time PCR assays were performed by using an Applied Biosystems StepOne qPCR instrument. In brief, the cDNA was synthesized from 1 μg of total RNA using M-MLV reverse transcriptase with an oligo(dT) primer. After cDNA synthesis, quantitative real-time PCR was performed in 5 μl of Fast SYBR® Green master mix. The primer sequences are as follows: mouse *ATG5* (NM_053069; 5'-TGCATCAAGTTCAGCTCTTCCT-3' and 3'-

CGCATCCTTGGATGGACAGT-3') and mouse *18S* (X00686; 5'-ACGGAAGGGCACCACCAGGA-3' and 5'-CACCACCACCCACGGAATCG-3'). The quantification of given genes was expressed as the mRNA levels normalized to a ribosomal housekeeping gene *18S* using the ΔΔCt method.

Detection of NEFA in medium

To determine the release of fatty acids from LD in 3T3-L1 cells, detection of NEFA in the medium was performed using 48-well tissue culture plates. Cells were differentiated into mature adipocyte and transfection with 100 pmol *ATG5* siRNA or control, followed by the treatment with vehicle (DMSO) or SFN (10 μM) for 24 h. After collecting the medium, NEFA content in the conditioned medium was measured with a commercial kit LabAssay^{TM} NEFA (Wako) according to the manufacture's protocol. The sample was mixed with reagent 1 and incubated at 37˚C for 10 min. Then, reagent 2 was added and after 10 min incubation at 37˚C, a colored product was formed with a maximal absorbance at 550 nm. The data were calibrated using the standard curve.

Statistical analysis

Data were collected from more than 2 independent experiments and were reported as the means ± S.E.M. Statistical analysis for 2-group comparison was performed using a 2-tailed Student's *t*–test, or one-way ANOVA with a Student-Newman post-hoc test for multi-group comparison. All data analysis was performed using GraphPad Prism 5 software (Graphpad Software, San Diego, CA, USA). $p < 0.05$ was considered statistically significant.

Results

SFN increases the LC3 expression in 3T3-L1 adipocytes

Investigation of the cytotoxic the effects of SFN (10 and 100 μM) in cells revealed a significant reduction in cell viability by administration of 100 μM SFN in differentiated 3T3-L1 cells for 10 days, unlike 10 μM SFN (**Supplementary Fig. 1**). For this reason, we subsequently used 10 μM SFN to determine the effects of SFN on lipolysis in adipocytes. No differences were noted in the number of LDs in 3T3-L1 cells between SFN treatment and DMSO (Control); however, rapamycin, an autophagy inducer, increased the number of LDs above that in the untreated controls. A reduction in LD size/LD number was also elicited in differentiated 3T3-L1 cells by treatment with SFN or rapamycin compared with controls (**Fig. 1A, B**). We next investigated the time-dependent effects of SFN on the LC3 expression in differentiated 3T3-L1 cells. LC3-II protein expression has been reported to increase in human prostate cancer cells after 6, 9, and 16 h of treatment with SFN [38]. For this reason, we deemed a time of up to 9 h to be appropriate for the evaluation of SFN effects on autophagy in 3T3-L1 cells. Differentiated 3T3-L1 cells were treated with 10 μM SFN for up to 9 h. Western blotting revealed that the LC3-II protein expression increased after 6 to 9 h of treatment with SFN. Conversely, SFN significantly reduced the protein levels of p62, a cargo receptor for autophagic degradation, after 3 to 9 h of treatment (**Fig. 1C, D**). Furthermore, we examined the relationship between LC3 and LDs in adipocytes by immunofluorescent staining for LC3 and BODIPY, a dye that stains neutral lipids in the LDs. Immunofluorescence showed that the LC3 expression was increased and co-localized with LDs in differentiated 3T3-L1 cells following SFN treatment for 3 h (**Fig. 1E, F**).

SFN increases the LC3 expression in the epididymal fat of obese mice

Mice were also fed an HFD or CFD for 8 weeks and then treated with SFN at 30 mg/kg body weight for 3 h to determine *in vivo* the regulation of lipolysis by SFN-mediated autophagy. SFN did not change the fasting plasma TG or NEFA levels in either the CFD or HFD group (**Table 1**). Western blotting demonstrated an upregulation of Nrf2 protein expression by SFN treatment in the epididymal fat of both groups. SFN significantly increased the expression of LC3-II protein (LC3-II/β-actin and LC3-II/LC3-I) in the epididymal fat of the HFD group but had no effect on epididymal fat in the CFD group. However, SFN did not significantly decrease the p62 protein levels in the epididymal fat in either group, in contrast to the results from the *in vitro* experiments (**Fig. 2A, B**).

The LDs in adipocytes of mammals are coated with perilipins, proteins from a gene family that includes five members (PLIN1−5). Perilipin-1 is the most abundant protein coating LDs and is considered essential for the formation and maturation of LDs and the storage of fatty acids released from TGs in the LDs [39]. Therefore, we investigated the colocalization of perilipin-1 and LC3 in adipocytes using immunofluorescent staining. LC3 expression was increased and LC-3 co-localized with perilipin in adipocytes following SFN treatment in the HFD group, but these effects were not seen in the CFD group (**Fig. 2C, D**).

SFN induces autophagy in 3T3-L1 adipocytes

As shown in Figure 1 and 2, we confirmed that SFN increases LC3-II protein expression in adipocytes. To

exclude the possibility that the increased LC3-II levels were resulted from the accumulation of LC3-II due to downstream inhibition other than SFN induction, we treated differentiated 3T3-L1 cells with SFN in the presence of lysosomal inhibitor Bafilomycin. SFN up-regulated additively to the LC3-II levels induced by Bafilomycin in mature 3T3-L1 cells for 6 h (**Fig. 3A**). Next, we analyzed the autophagy flux in differentiated 3T3-L1 cells using a tandem mCherry-EGFP-LC3 reporter fluorescence assay. LC3-attached autophagosomes are known to be formed in the cytoplasm when autophagy is induced, fusing with endosomes or lysosomes to form autolysosomes, which provide an acidic environment and digestive function to the interior of the autophagosome. mCherry is acid-stable, while GFP is acid-labile; therefore, if autophagic flux is increased, both yellow and red punctate are increased. However, if autophagosome maturation into autolysosomes is blocked, only yellow punctate is increased without a concomitant increase in red punctate (**Fig. 3B**). After stable 3T3-L1 cells expressing mCherry-EGFP-LC3 were differentiated into mature adipocytes, they were treated with vehicle (DMSO), Bafilomycin, or SFN for 3 h. While Bafilomycin treatment increased yellow puncta, SFN induced red puncta compared with controls in adipocytes (**Fig. 3C**).

To further confirm the effects of SFN on the autophagy flux, we next used another autophagy flux assay probe, the GFP-LC3-RFP-LC3ΔG [36]. The probe is cleaved by Atg4 under autophagy induction and divided into GFP-LC3 and RFP-LC3ΔG. GFP-LC3 conjugates with PE on an isolation membrane through the glycine 120 residue. After autophagosome-lysosome fusion, the interior GFP-LC3 is degraded, and GFP fluorescence is diminished by the acidic environment of the autolysosome. Because RFP-LC3ΔG cannot be degraded because of its inability to

conjugate PE due to the deletion of 120, RFP fluorescence can be used as internal control due to its stability. A decline in the GFP/RFP ratio indicates autophagic flux (**Fig. 3D**). 3T3-L1 cells stably expressing GFP-LC3-RFP-LC3ΔG were treated with 10 μM SFN for 3 h. Treatment with SFN significantly decreased the GFP/RFP ratio compared with control (**Fig. 3E**). These results indicate that SFN blocks autophagic flux, resulting in the significant degradation of autophagic substrates, such as LC3-II, in 3T3-L1 adipocytes.

SFN induces activation of the AMPK-mTOR-ULK1 signaling pathway in 3T3-L1 adipocytes

To clarify the contribution of SFN to lipophagy in adipocytes, we generated mature 3T3-L1 cells with the knockdown of *ATG5*. As expected, *ATG5*-specific siRNA reduced the endogenous *ATG5* mRNA levels by more than 60% along with the LC3-II protein expression downstream of the ATG12-ATG5-ATG16 complex in 3T3-L1 adipocytes (**Fig. 4A, B**). *ATG5*-knockdown 3T3-L1 adipocytes and control 3T3-L1 adipocytes were treated with SFN or DMSO for 10 days. Subsequent oil red-O staining showed that *ATG5* knockdown partially blocked the SFN-induced reduction in the LD size in 3T3-L1 adipocytes (**Fig. 4C, D**). We also investigated the rapid effect of SFN on the release of NEFA from LDs in 3T3-L1 adipocytes treated with *ATG5*-specific siRNA. SFN significantly increased the release of NEFA from LDs in mature 3T3-L1 adipocytes, but *ATG5*-knockdown inhibited the effect induced by SFN treatment (**Fig. 4E**).

Autophagy is elicited in cells through the induction of ULK1 *via* the phosphorylation of AMPK or the inhibited mTOR [10, 11]. Indeed, it has been reported that SFN provoked autophagy through the AMPK-mTOR-ULK1

signaling pathway in hepatocytes [40]. To investigate the mechanisms underlying the induction of autophagy by SFN in 3T3-L1 adipocytes, we examined the AMPK-mTOR-ULK1 signaling pathway using western blotting. Differentiated 3T3-L1 cells were treated with 10 μM SFN for up to 9 h. We confirmed that SFN increased the amount of nuclear Nrf2 protein after 0.5 to 9 h treatment (**Fig. 5C, D**). Elevated levels phosphorylated-AMPKα (p-AMPKα) and phosphorylated-ULK1 (p-ULK1) levels were transiently induced after 1 h of SFN treatment. Following the induction of p-AMPKα, SFN reduced the phosphorylated-mTOR (p-mTOR) levels from 1 to 6 h of treatment. The levels of phosphorylated-4E-BP1 (p-4E-BP1), an mTOR substrate, were transiently reduced after 1 to 3 h of SFN treatment (**Fig. 5A, B**). We also investigated whether autophagy pathways other than the AMPK-mTOR-ULK1 pathway might be involved in the induction of autophagy by SFN in 3T3-L1 adipocytes [21, 41]. SFN treatment did not affect the phosphorylation or protein expression of component of the ERK pathway (ERK1/2) or the Rubicon pathway (Rubicon protein) in 3T3-L1 adipocytes (**Fig. 5C, D**).

To clarify the effect of the AMPK-mTOR-ULK1 signaling pathway on lipophagy in adipocytes, we generated mature 3T3-L1 cells with the knockdown of *AMPKα1/2*. As expected, *AMPKα1/2*-specific siRNA reduced the endogenous phosphorylated AMPKα (p-AMPKα) and total AMPKα (AMPKα) protein levels in 3T3-L1 adipocytes (**Fig. 5E**). We also confirmed that *AMPKα1/2*-knockdown significantly decreased the release of NEFA from LDs in mature 3T3-L1 adipocytes induced by SFN treatment (**Fig. 5F**). These data suggest that SFN enhanced autophagy through the AMPK-mTOR-ULK1 signaling pathway in differentiated 3T3-L1 cells (**Fig. 5G**).

Discussion

In the present study, we determined that SFN contributes to lipophagy in adipocytes of mice fed an HFD and induces lipophagy through the AMPK-mTOR-ULK1 signaling pathway in differentiated 3T3-L1 cells. Recently, it has been suggested that lipophagy can contribute to lipolysis in adipocytes [19−22]. While dietary factors regulate lipolysis through various pathways in adipose tissue [4−7], the effects of dietary factors on lipophagy in adipocytes remain unclear. SFN also regulates lipolysis in 3T3-L1 adipocytes via HSL activation and adipocytes browning [7, 34]. However, the regulation of lipolysis by SFN in adipocytes focused on lipophagy, but not lipase and adipocyte browning, has not yet been identified. In the present study, we found that a 3 h treatment with SFN increased the expression of LC3-II protein in the epididymal fat of mice fed an HFD but not a CFD. Immunofluorescent staining showed that SFN treatment increased the expression of LC3 and its co-localized with perilipin, an adipocyte-specific protein that covers the surface of LDs, in adipocytes of the HFD group but not the CFD group. These results suggest that the effects of SFN on autophagy in adipocytes vary depending on the consumption of diets with different fat content. We consider that this variation may reflect differences in the method of administration of SFN to the mice. The mice fed have larger amounts of abdominal fat, including epididymal fat when fed the HFD than the CFD, and the administered SFN may be delivered more rapidly to epididymal fat. If the method of SFN administration is changed from intraperitoneal to oral administration, this difference in SFN effects on autophagy in the adipocytes between the CFD and HFD groups may not be observed. In differentiated 3T3-L1 cells, we showed that SFN-induced lipolysis and transiently increased the expression of LC3-II protein while also increasing the accumulation

of LC3 co-localized with LDs. We also demonstrated that SFN can induce autophagy in differentiated 3T3-L1 cells using a mCherry-EGFP-LC3 or GFP-LC3-RFP-LC3ΔG vector. In addition, we confirmed that *ATG5* knockdown partially blocked the SFN-induced reduction in the LD size and SFN-induced increase in the release of NEFA from LDs in 3T3-L1 adipocytes. These results suggest that SFN can regulate autophagy in murine adipose both *in vitro* and *in vivo*.

Because p62 acts as a cargo receptor for the autophagic degradation of ubiquitinated targets, the induction of autophagy generally down-regulates p62 protein levels [29, 42]. Indeed, p62 protein levels are decreased by the increase in autophagy flux through cAMP/PKA signaling and nutrient starvation in adipocytes differentiated from C3H10T1/2 cells [20]. Mice with knockout of adipocyte-specific Beclin-1, which plays a central role in autophagy, show increased p62 protein levels, resulting in defective β_3-adrenergic receptor agonist-induced lipolysis in adipose tissue [20]. In the present study, western blotting revealed significant reductions in p62 protein levels in differentiated 3T3-L1 cells after 3 to 9 h of treatment with SFN. However, unlike its effects *in vitro*, SFN did not promote a significant decrease in p62 protein levels in the epididymal fat of either the CFD or HFD mouse groups. The expression of the *p62* gene is well known to be induced by Nrf2 binding to the ARE of its gene promoter [43]. Nrf2 activation induces p62, which competitively inhibits the Keap1-Nrf2 interaction and binds to Keap1, resulting in the induction of autophagy and the degradation of p62 [30−32]. Indeed, we recently demonstrated that many polyphenolic flavonoids (Nrf2 activators) up-regulate p62, which might play a common role in the pro-autophagic effects of phytochemicals in Caco-2 cells [44]. Taken together, these results indicate that if SFN had been

administered to mice for longer than 3 h, the p62 protein levels might have decreased in the epididymal adipose tissues.

SFN induces antiobesity activity by inhibiting lipogenesis through the down-regulation of PPARγ and activation of the AMPK pathway [45]. In addition, the AMPK-mTOR pathway is known to modulate autophagy via the coordinated phosphorylation of ULK1 [10, 11]. In the present study, SFN quickly and transiently increased the p-AMPKα and p-ULK1 levels and reduced the p-mTOR levels in differentiated 3T3-L1 cells. Furthermore, the levels of p-4E-BP1, an mTOR substrate, were transiently reduced by SFN treatment. We also confirmed that *AMPKα1/2*-knockdown significantly decreased the release of NEFA from LDs in mature 3T3-L1 adipocytes induced by SFN treatment. Although some pathways, such as the ERK and Rubicon pathways, are also involved in autophagy regulation [21, 41], we confirmed that SFN did not affect the phosphorylation of ERK1/2 and Rubicon protein expression levels in 3T3-L1 adipocytes. These results suggest that SFN triggers autophagy through the AMPK-mTOR-ULK1 signaling pathway in differentiated 3T3-L1 cells. Yang *et al*. reported a similar observation in hepatocytes but not adipocytes [40]. They found that SFN prevented HFD-induced non-alcoholic fatty liver disease (NAFLD) in mice via the down-regulation of the NOD-like receptor family pyrin domain containing 3 (NLRP3) inflammasome through AMPK-dependent autophagy in the liver. However, the levels of saturated fatty acid (SFA), such as palmitate, in plasma are reportedly elevated in NAFLD patients, which promotes an inflammatory response by directly engaging Toll-like receptors and inducing the NF-κB-dependent production of inflammatory cytokines [46−48]. Yang *et al*. also suggested that SFN inhibited the SFA-induced activation of the NLRP3 inflammasome in

primary mouse hepatocytes [40]. We recently reported that SFA can perturb the autophagy machinery in vascular smooth muscle cells, contributing to vascular calcification and apoptosis [42]. Taken together, these reports suggest that SFN ameliorates NAFLD through the improvement of SFA-induced autophagy inhibition in hepatocytes.

The present findings suggest that the AMPK-mTOR-ULK1 signaling pathway is involved in the mechanism underlying the lipophagy induced by SFN in 3T3-L1 adipocytes. Sirtuin 1 (Sirt1) is well recognized as a major regulator of autophagy and directly regulates autophagy through the deacetylation of several mediator proteins of autophagy, such as ATG5, ATG7, and LC3 [49]. Interestingly, SFN increases the expression of Sirt1 and PPARγ coactivator 1 alpha (PGC-1α), a downstream target of Sirt1, in 3T3-L1 mature adipocytes [34]. Interestingly, resveratrol, a Sirt1 activator, can stimulate AMPK action through a Sirt1-dependent mechanism [50]. We therefore considered that SFN can activate the AMPK signal through Sirt1 and promote lipophagy in 3T3-L1 cells. Indeed, we confirmed an increase in Sirt1 protein expression in differentiated 3T3-L1 cells after a 1 h treatment with SFN (**Supplementary Fig. 2**). In addition, Sirt1 activates transcription factor EB (TFEB), a master regulator of autophagic and lysosomal functions [51, 52]. Recently, Li *et al*. suggested that SFN increases autophagosome and lysosome biogenesis through a TFEB-mediated lysosome-dependent transcriptional program in HeLa cells [53]. Although the present findings suggest the effects of SFN on lipophagy through the AMPK-mTOR-ULK1 signaling pathway, we cannot deny the probable presence of SFN-induced lipophagy via Sirt1-AMPK and Sirt1-TFEB in adipocytes.

In conclusion, the present study showed that the LC3 expression was increased and co-localized with perilipin

in adipocytes of mice fed an HFD following SFN treatment. Furthermore, SFN was shown to induce lipophagy through the AMPK-mTOR-ULK1 signaling pathway in adipocytes, resulting in the reduction of LDs. To our knowledge, this is the first study to demonstrate that dietary factors partially contribute to lipolysis thorough lipophagy in adipocytes.

Acknowledgments: We thank Dr. J. Debnath (University of California San Francisco) for providing pBABE-puro mCherry-EGFP-LC3 plasmid, Dr. N. Mizushima (The University of Tokyo) for providing pMRX-IP-GFP-LC3-RFP-LC3ΔG plasmid. for technical assistance. We also thank Fujii Memorial Institute of Medical Science, Support Center for Advanced Medical Sciences, Tokushima University Graduate School of Biomedical Sciences, Dr. Y. Niida, R. Kawashima, S. Aoyagi, and M. Fujimoto (Department of Clinical Nutrition and Food Management, Institute of Biomedical Sciences, Tokushima University Graduate School) for technical assistance.

Declarations of interest: The authors declare that they have no conflicts of interest with the contents of this article.

References

1. Kopelman PG. Obesity as a medical problem. Nature 2000;404:635-43.
2. Heymsfield SB, Wadden TA. Mechanisms, Pathophysiology, and Management of Obesity. N Engl J Med 2017;376:254-66.
3. Bray GA. A concise review on the therapeutics of obesity. Nutrition 2000;16:953-60.
4. Abuduli M, Ohminami H, Otani T, Kubo H, Ueda H, Kawai Y, et al. Effects of dietary phosphate on glucose and lipid metabolism. Am J Physiol Endocrinol Metab 2016;310:E526-38.
5. Imi Y, Yabiki N, Abuduli M, Masuda M, Yamanaka-Okumura H, Taketani Y. High phosphate diet suppresses lipogenesis in white adipose tissue. J Clin Biochem Nutr 2018;63:181-91.
6. Liu CW, Tsai HC, Huang CC, Tsai CY, Su YB, Lin MW, et al. Effects and mechanisms of caffeine to improve immunological and metabolic abnormalities in diet-induced obese rats. Am J Physiol Endocrinol Metab 2018;314:E433-47.
7. Lee JH, Moon MH, Jeong JK, Park YG, Lee YJ, Seol JW, et al. Sulforaphane induced adipolysis via hormone sensitive lipase activation, regulated by AMPK signaling pathway. Biochem Biophys Res Commun 2012;426:492-7.
8. Duncan RE, Ahmadian M, Jaworski K, Sarkadi-Nagy E, Sul HS. Regulation of lipolysis in adipocytes. Annu Rev Nutr 2007;27:79-101.
9. Singh R, Kaushik S, Wang Y, Xiang Y, Novak I, Komatsu M, et al. Autophagy regulates lipid

metabolism. Nature 2009;458:1131-5.

10. Jung CH, Ro SH, Cao J, Otto NM, Kim DH. mTOR regulation of autophagy. FEBS Lett 2010;584:1287-95.

11. Kim J, Kundu M, Viollet B, Guan KL. AMPK and mTOR regulate autophagy through direct phosphorylation of Ulk1. Nat Cell Biol 2011;13:132-41.

12. Mihaylova MM, Shaw RJ. The AMPK signalling pathway coordinates cell growth, autophagy and metabolism. Nat Cell Biol 2011;13:1016-23.

13. Fujita N, Itoh T, Omori H, Fukuda M, Noda T, Yoshimori T. The Atg16L complex specifies the site of LC3 lipidation for membrane biogenesis in autophagy. Mol Biol Cell 2008;19:2092-100.

14. Ichimura Y, Kirisako T, Takao T, Satomi Y, Shimonishi Y, Ishihara N, et al. A ubiquitin-like system mediates protein lipidation. Nature 2000;408:488-92.

15. Kabeya Y, Mizushima N, Yamamoto A, Oshitani-Okamoto S, Ohsumi Y, Yoshimori T. LC3, GABARAP and GATE16 localize to autophagosomal membrane depending on form-II formation. J Cell Sci 2004;117:2805-12.

16. Matsushita M, Suzuki NN, Obara K, Fujioka Y, Ohsumi Y, Inagaki F. Structure of Atg5.Atg16, a complex essential for autophagy. J Biol Chem 2007;282:6763-72.

17. Mizushima N, Kuma A, Kobayashi Y, Yamamoto A, Matsubae M, Takao T, et al. Mouse Apg16L, a novel WD-repeat protein, targets to the autophagic isolation membrane with the Apg12-Apg5 conjugate. J

Cell Sci 2003;116:1679-88.

18. Tanida I, Sou YS, Ezaki J, Minematsu-Ikeguchi N, Ueno T, Kominami E. HsAtg4B/HsApg4B/autophagin-1 cleaves the carboxyl termini of three human Atg8 homologues and delipidates microtubule-associated protein light chain 3- and GABAA receptor-associated protein-phospholipid conjugates. J Biol Chem 2004;279:36268-76.

19. Lizaso A, Tan KT, Lee YH. β-adrenergic receptor-stimulated lipolysis requires the RAB7-mediated autolysosomal lipid degradation. Autophagy 2013;9:1228-43.

20. Son Y, Cho YK, Saha A, Kwon HJ, Park JH, Kim M, et al. Adipocyte-specific Beclin1 deletion impairs lipolysis and mitochondrial integrity in adipose tissue. Mol Metab 2020;39:101005.

21. Yamamuro T, Kawabata T, Fukuhara A, Saita S, Nakamura S, Takeshita H, et al. Age-dependent loss of adipose Rubicon promotes metabolic disorders via excess autophagy. Nat Commun 2020;11:4150.

22. Ogasawara Y, Cheng J, Tatematsu T, Uchida M, Murase O, Yoshikawa S, et al. Long-term autophagy is sustained by activation of CCTβ3 on lipid droplets. Nat Commun 2020;11:4480.

23. Zhang Y, Talalay P, Cho CG, Posner GH. A major inducer of anticarcinogenic protective enzymes from broccoli: isolation and elucidation of structure. Proc Natl Acad Sci U S A 1992;89:23992403.

24. Kensler TW, Wakabayashi N, Biswal S. Cell survival responses to environmental stresses via the Keap1-Nrf2-ARE pathway. Annu Rev Pharmacol Toxicol 2007;47:89-116.

25. Negrette-Guzman M, Huerta-Yepez S, Tapia E, Pedraza-Chaverri J. Modulation of mitochondrial

functions by the indirect antioxidant sulforaphane: a seemingly contradictory dual role and an integrative hypothesis. Free Radic Biol Med 2013;65:1078-89.

26. Itoh K, Wakabayashi N, Katoh Y, Ishii T, Igarashi K, Engel JD, et al. Keap1 represses nuclear activation of antioxidant responsive elements by Nrf2 through binding to the amino-terminal Neh2 domain. Genes Dev 1999;13:76-86.

27. Kobayashi A, Kang MI, Okawa H, Ohtsuji M, Zenke Y, Chiba T, et al. Oxidative stress sensor Keap1 functions as an adaptor for Cul3-based E3 ligase to regulate proteasomal degradation of Nrf2. Mol Cell Biol 2004;24:7130-9.

28. Zhang DD, Lo SC, Cross JV, Templeton DJ, Hannink M. Keap1 is a redox-regulated substrate adaptor protein for a Cul3-dependent ubiquitin ligase complex. Mol Cell Biol 2004;24:10941-53.

29. Bjørkøy G, Lamark T, Brech A, Outzen H, Perander M, Overvatn A, et al. p62/SQSTM1 forms protein aggregates degraded by autophagy and has a protective effect on huntingtin-induced cell death. J Cell Biol 2005;171:603-14.

30. Ichimura Y, Waguri S, Sou YS, Kageyama S, Hasegawa J, Ishimura R, et al. Phosphorylation of p62 activates the Keap1-Nrf2 pathway during selective autophagy. Mol Cell 2013;51:618-31.

31. Komatsu M, Kurokawa H, Waguri S, Taguchi K, Kobayashi A, Ichimura Y, et al. The selective autophagy substrate p62 activates the stress responsive transcription factor Nrf2 through inactivation of Keap1. Nat Cell Biol 2010;12:213-23.

32. Lau A, Wang XJ, Zhao F, Villeneuve NF, Wu T, Jiang T, et al. A noncanonical pbs of Nrf2 activation by autophagy deficiency: direct interaction between Keap1 and p62. Mol Cell Biol 2010;30: 3275-85.

33. Martinez-Lopez N, Garcia-Macia M, Sahu S, Athonvarangkul D, Liebling E, Merlo P, et al. Autophagy in the CNS and Periphery Coordinate Lipophagy and Lipolysis in the Brown Adipose Tissue and Liver. Cell Metab 2016;23:113-27.

34. Zhang HQ, Chen SY, Wang AS, Yao AJ, Fu JF, Zhao JS, et al. Sulforaphane induces adipocyte browning and promotes glucose and lipid utilization. Mol Nutr Food Res 2016;60:2185-97.

35. N'Diaye EN, Kajihara KK, Hsieh I, Morisaki H, Debnath J, Brown EJ. PLIC proteins or ubiquilins regulate autophagy-dependent cell survival during nutrient starvation. EMBO Rep 2009;10:173-9.

36. Kaizuka T, Morishita H, Hama Y, Tsukamoto S, Matsui T, Toyota Y, et al. An Autophagic Flux Probe that Releases an Internal Control. Mol Cell 2016;64:835-49.

37. Masuda M, Yamamoto H, Takei Y, Nakahashi O, Adachi Y, Ohnishi K, et al. All-trans retinoic acid reduces the transcriptional regulation of intestinal sodium-dependent phosphate co-transporter gene (Npt2b). Biochem J 2020;477: 817-31.

38. Herman-Antosiewicz A, Johnson DE, Singh SV. Sulforaphane causes autophagy to inhibit release of cytochrome C and apoptosis in human prostate cancer cells. Cancer Res 2006;66: 5828-35.

39. Brasaemle DL, Subramanian V, Garcia A, Marcinkiewicz A, Rothenberg A. Perilipin A and the control of triacylglycerol metabolism. Mol Cell Biochem 2009;326:15-21.

40. Yang G, Lee HE, Lee JY. A pharmacological inhibitor of NLRP3 inflammasome prevents non-alcoholic fatty liver disease in a mouse model induced by high fat diet. Sci Rep 2016;6:24399.

41. Janku F, McConkey DJ, Hong DS, Kurzrock R. Autophagy as a target for anticancer therapy. Nat Rev Clin Oncol 2011;8: 528-39.

42. Shiozaki Y, Miyazaki-Anzai S, Okamura K, Keenan AL, Masuda M, Miyazaki M. GPAT4-Generated Saturated LPAs Induce Lipotoxicity through Inhibition of Autophagy by Abnormal Formation of Omegasomes. iScience 2020;23:101105.

43. Jain A, Lamark T, Sjøttem E, Larsen KB, Awuh JA, Øvervatn A, et al. p62/SQSTM1 is a target gene for transcription factor NRF2 and creates a positive feedback loop by inducing antioxidant response element-driven gene transcription. J Biol Chem 2010;285:22576-91.

44. Ohnishi K, Yano S, Fujimoto M, Sakai M, Harumoto E, Furuichi A, et al. Identification of Dietary Phytochemicals Capable of Enhancing the Autophagy Flux in HeLa and Caco-2 Human Cell Lines. Antioxidants (Basel) 2020;9:1193.

45. Choi KM, Lee YS, Kim W, Kim SJ, Shin KO, Yu JY, et al. Sulforaphane attenuates obesity by inhibiting adipogenesis and activating the AMPK pathway in obese mice. J Nutr Biochem 2014;25:201-7.

46. Puri P, Wiest MM, Cheung O, Mirshahi F, Sargeant C, Min HK, et al. The plasma lipidomic signature of nonalcoholic steatohepatitis. Hepatology 2009;50:1827-38.

47. Shi H, Kokoeva MV, Inouye K, Tzameli I, Yin H, Flier JS. TLR4 links innate immunity and fatty acid-

induced insulin resistance. J Clin Invest 2006;116:3015-25.

48. Wen H, Gris D, Lei Y, Jha S, Zhang L, Huang MT, et al. Fatty acid-induced NLRP3-ASC inflammasome activation interferes with insulin signaling. Nat Immunol 2011;12:408-15.

49. Lee IH, Cao L, Mostoslavsky R, Lombard DB, Liu J, Bruns NE, et al. A role for the NAD-dependent deacetylase Sirt1 in the regulation of autophagy. Proc Natl Acad Sci U S A 2008;105:3374-79.

50. Breen DM, Sanli T, Giacca A, Tsiani E. Stimulation of muscle cell glucose uptake by resveratrol through sirtuins and AMPK. Biochem Biophys Res Commun 2008;374: 117-22.

51. Sardiello M, Palmieri M, di Ronza A, Medina DL, Valenza M, Gennarino VA, et al. A gene network regulating lysosomal biogenesis and function. Science 2009;325:473-7.

52. Settembre C, Malta CD, Polito VA, Arencibia MG, Vetrini F, Erdin S, et al. TFEB links autophagy to lysosomal biogenesis. Science 2011;332:1429-33.

53. Li D, Shao R, Wang N, Zhou N, Du K, Shi J, et al. Sulforaphane Activates a lysosome-dependent transcriptional program to mitigate oxidative stress. Autophagy 2021;17:872-87.

Figure Legends

Fig. 1. Effects of SFN treatment on the expression of LC3 expression in 3T3-L1 adipocytes. (A, B) Differentiated 3T3-L1 cells were treated with SFN (100 μM), 500 nM rapamycin, or 0.1% DMSO (Control) for 10 days. Cells were then fixed, stained with oil red-O staining, and analyzed with a BZ-9000 fluorescence microscope. Lipid accumulation was quantified using the ImageJ imaging software program. Scale bar = 50 μm. Values are the mean ± S.E.M. (n = 9). *p < 0.001 vs. Control (one-way ANOVA with a Student-Newman post-hoc test). (C, D) Western blotting of LC3 and p62 in the 3T3-L1 adipocytes. Differentiated 3T3-L1 cells were treated with 10 μM SFN or 0.1% DMSO (Control) for the indicated periods (0, 0.5, 1, 3, 6, and 9 h). β-actin was used as an internal control. Values are the mean ± S.E.M. (n = 3). *p < 0.05 vs. 0 h (one-way ANOVA with a Student-Newman post-hoc test). (E, F) After differentiated 3T3-L1 cells were treated with 10 μM SFN or 0.1% DMSO (Control) for 3 h, cells were fixed and stained for LC3 Ab conjugated to Alexa Fluor 568 (red). LDs were stained with BODIPY (493/503). Images were taken with a confocal laser-scanning microscope. Percentage colocalization of LC3 with BODIPY. Scale bar = 10 μm. Values are the mean ± S.E.M. (n = 3). *p < 0.05 (two-tailed unpaired Student's t test).

Fig. 2. Effects of SFN treatment on the expression of LC3 in epididymal fat of obese mice. Seven-week-old male mice were fed a high-fat diet (HFD) or control-fat diet (CFD) for 8 weeks. After fasting for 18 h, the mice were randomly divided into 2 groups and treated with DMSO (Control) or SFN for 3 h. (A, B) Western blotting of LC3 and p62 in epididymal fat. β-actin was used as an internal control. (C, D) LC3 Ab and a secondary Ab conjugated to Alexa fluor 555 (red), and Perilipin Ab and a secondary Ab conjugated to Alexa Fluor 488 (green). Nuclear staining with DAPI is shown in blue. Images were taken with a fluorescence microscope. Percentage colocalization of LC3 with perilipin. Scale bar = 100 μm. Values are the mean ± S.E.M. (n = 4). *p < 0.05 (two-tailed unpaired Student's t test).

Fig. 3. Effects of SFN on the autophagy flux in 3T3-L1 adipocytes. (A) Western blotting of LC3 in 3T3-L1 adipocytes. Differentiated 3T3-L1 cells were treated with 10 μM SFN with or without 100 nM Bafilomycin (BAF), or 0.1% DMSO (Control) for 6 h. β-actin was used as an internal control. (B) Schematic illustration of the tandem mCherry-EGFP-LC3 plasmid. (C) Differentiated 3T3-L1 cells stably expressing mCherry-EGFP-LC3 were treated with 10 μM SFN, 100 nM Bafilomycin (BAF), or 0.1% DMSO for 3 h. Scale bar = 50 μm. (D) Schematic illustration of the measurement of autophagic flux with a GFP-LC3-RFP-ΔG probe. (E) Differentiated 3T3-L1 cells stably expressing GFP-LC3-RFP-ΔG were treated with SFN (10 μM) or 0.1% DMSO (Control) for 3 h. GFP/RFP ratio data were expressed as the fold-value against controls. Scale bar = 50 μm. Values are the mean ± S.E.M. (n = 4). *p < 0.05, **p < 0.01 (one-way ANOVA with a Student-Newman post-hoc test).

Fig. 4. Effects of *ATG5*-knockdown on the SFN-induced cutdown of LDs in 3T3-L1 adipocytes. (A) Endogenous *ATG5* mRNA and (B) LC3 protein were detected by real-time PCR and western blotting 48 h after

transfection with 100 pmpl *ATG5* siRNA (siATG5) or negative control (siCont.) in differentiated 3T3-L1 cells. Values are the mean ± S.E.M. (n = 3). *p < 0.05 (two-tailed unpaired Student's t test). (C, D) Differentiated 3T3-L1 cells were treated with 10 μM SFN or DMSO (control) for 10 days after transfection with 100 pmol *ATG5* siRNA or negative control. Cells were then fixed, stained with oil red-O staining, and analyzed with a BZ-9000 fluorescence microscope. Lipid accumulation was quantified using the ImageJ imaging software program. Scale bar = 50 μm. Values are the mean ± S.E.M. (n = 10). (E) Differentiated 3T3-L1 cells were treated with 10 μM SFN for DMSO (control) 24 h after transfection with 100 pmol *ATG5* siRNA or negative control. The culture medium was collected and assayed for NEFA content (mEq/L/mg protein). Values are the mean ± S.E.M. (n = 9−12). *p < 0.05 (one-way ANOVA with a Student-Newman post-hoc test).

Fig. 5. Induction of autophagy by SFN through the AMPK pathway in 3T3-L1 adipocytes. Differentiated 3T3-L1 cells were treated with 10 μM SFN at the indicated time (0, 0.5, 1, 3, 6, and 9 h). (A, B) The expression of phosphorylated AMPKα (p-AMPKα), total AMPKα (AMPKα), phosphorylated mTOR (p-mTOR), total mTOR (mTOR), phosphorylated ULK1 (p-ULK1), total ULK1 (ULK1), phosphorylated 4E-BP1 (p-4E-BP1), total 4E-BP1 (4E-BP1), (C, D) phosphorylated ERK1/2 (p-ERK1/2), total ERK1/2 (ERK1/2), Rubicon protein, and nuclear Nrf2 protein were determined by western blotting with specific antibodies. β-actin or Histone H3 was used as an internal control. Values are the mean ± S.E.M. (n = 3). *p < 0.05 vs. 0 h (one-way ANOVA with a Student-Newman post-hoc test). (E, F) Differentiated 3T3-L1 cells were treated with 10 μM SFN for DMSO (control) 24 h after transfection with 100 pmol *AMPKα1/2* siRNA (siAMPKα) or negative control (siCont.) for 24 h. (E) The expression of p-AMPKα and AMPKα protein were determined by western blotting with specific antibodies. (F) The culture medium was collected and assayed for NEFA content (mEq/L/mg protein). Values are the mean ± S.E.M. (n = 4). *p < 0.05 (one-way ANOVA with a Student-Newman post-hoc test). (G) Schematic illustration of the induction of lipophagy by SFN in 3T3-L1 adipocytes.

Supplementary Figure Legends

Figure S1. Effects of SFN on cell viability in mature 3T3-L1 cells.

Differentiated 3T3-L1 cells were treated with SFN (10 and 100 μM) or 0.1% DMSO (Control) for 10 days. Cell survival was tested using a CellTiter-Fluor™ Cell Viability Assay. The fluorescence spectra were measured using SpectraMax i3 with a filter set at Ex/Em 390/505 nm. Values are the mean ± S.E.M. (n = 9). *p < 0.05 vs. Control (one-way ANOVA with a Student-Newman post-hoc test).

Figure S2. Effects of SFN on the expression of Sirt1 in mature 3T3-L1 cells.

Differentiated 3T3-L1 cells were treated with SFN (100 μM) at the indicated time (0, 0.5, and 1 h). (A, B) The expression of Sirt1 protein was determined by western blotting with specific antibodies. β-actin was used as an internal control. Values are the mean ± S.E.M. (n = 3). *p < 0.05 (one-way ANOVA with a Student-Newman post-hoc test).

Figure. 1 Masuda M. et al

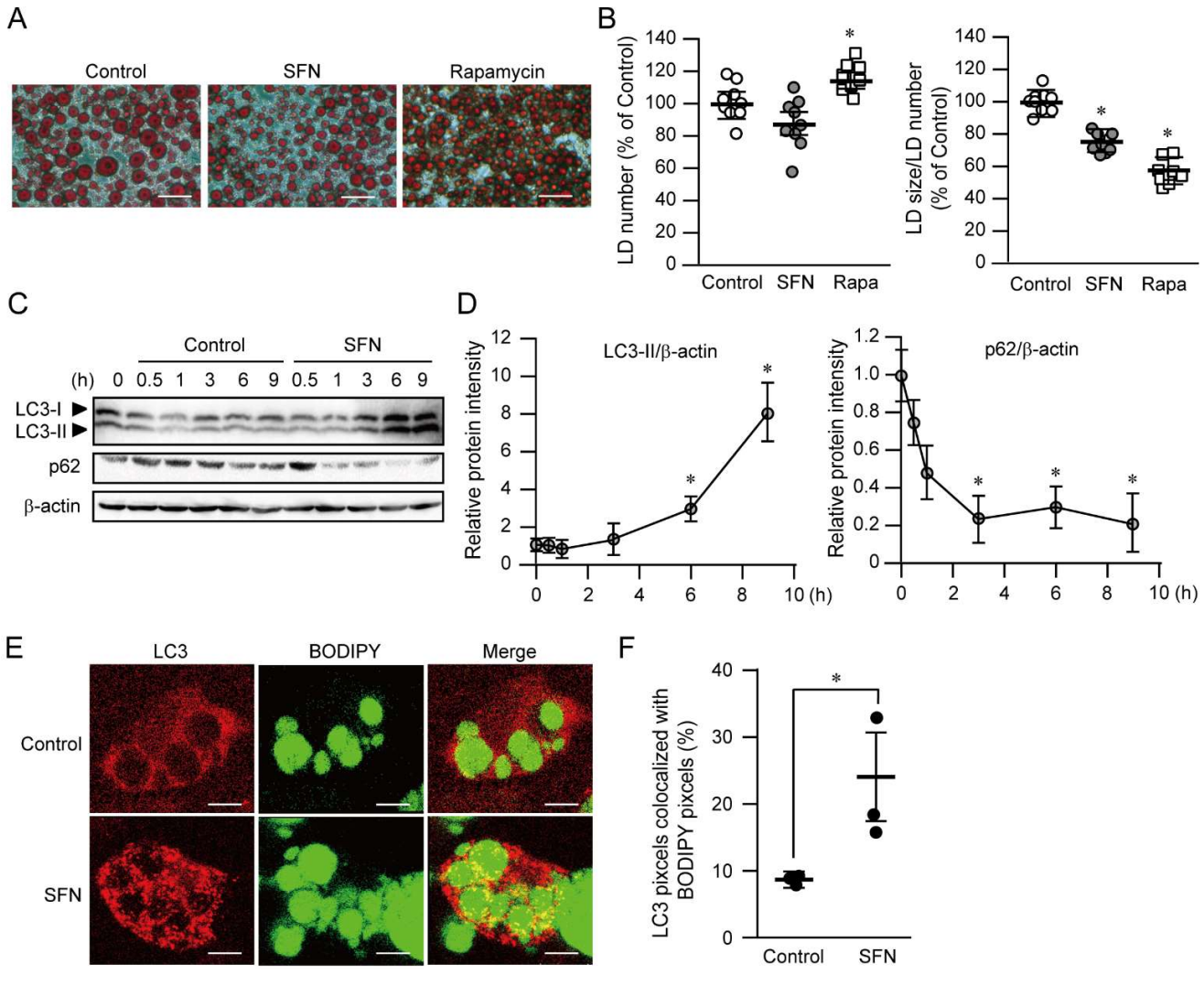

Figure. 2 Masuda M. et al

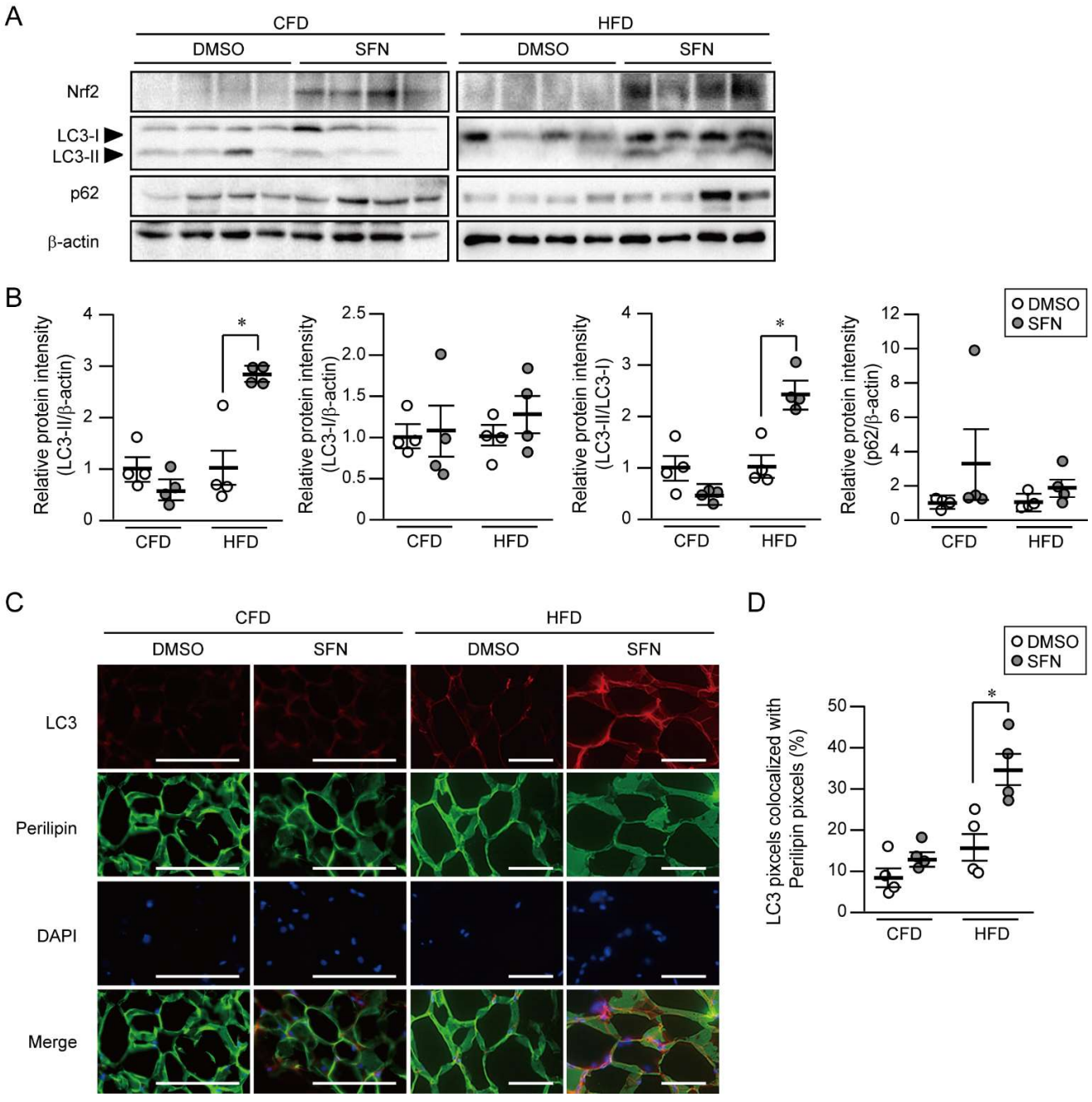

Figure. 3 Masuda M. et al

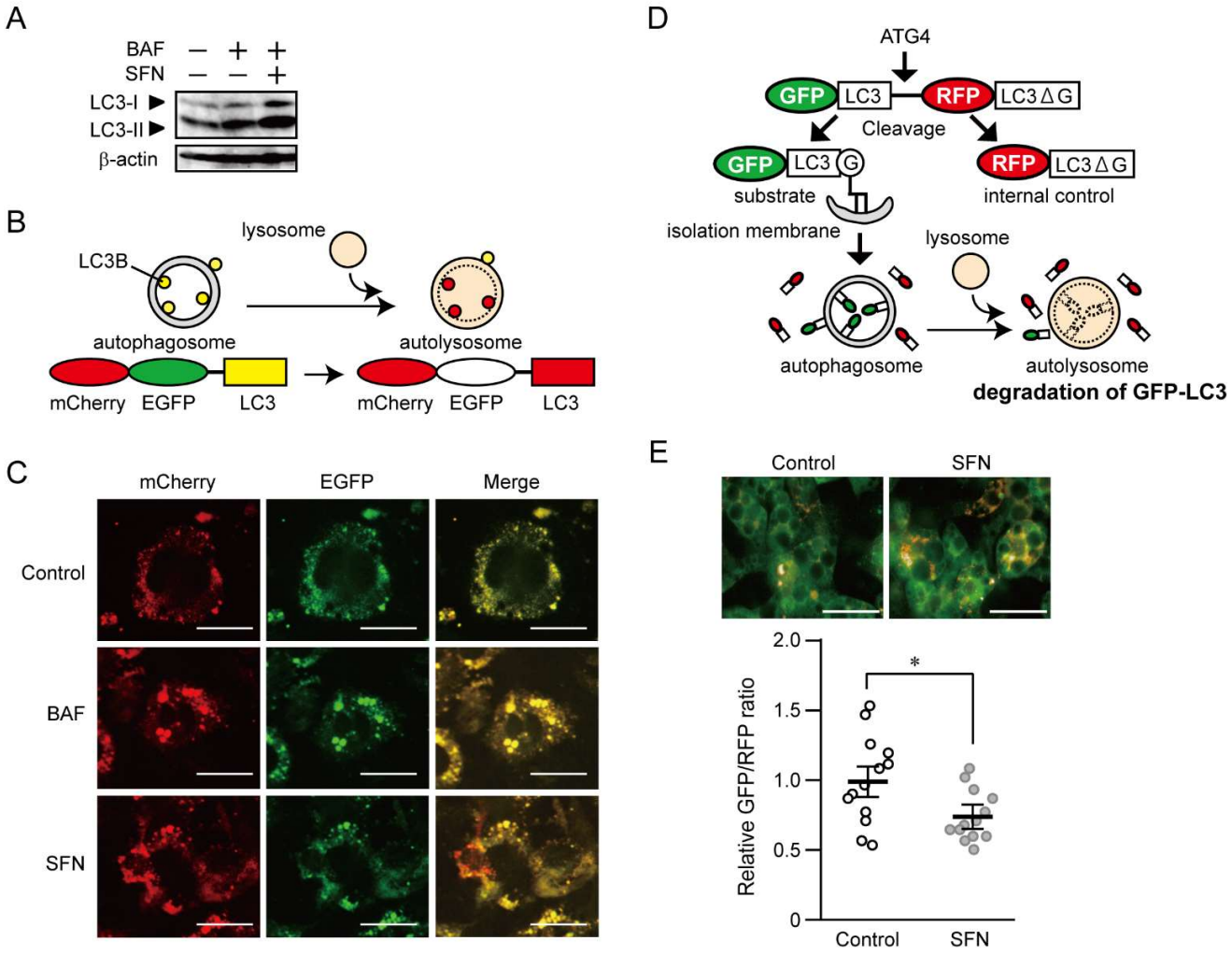

1

2

Figure. 4 Masuda M. et al

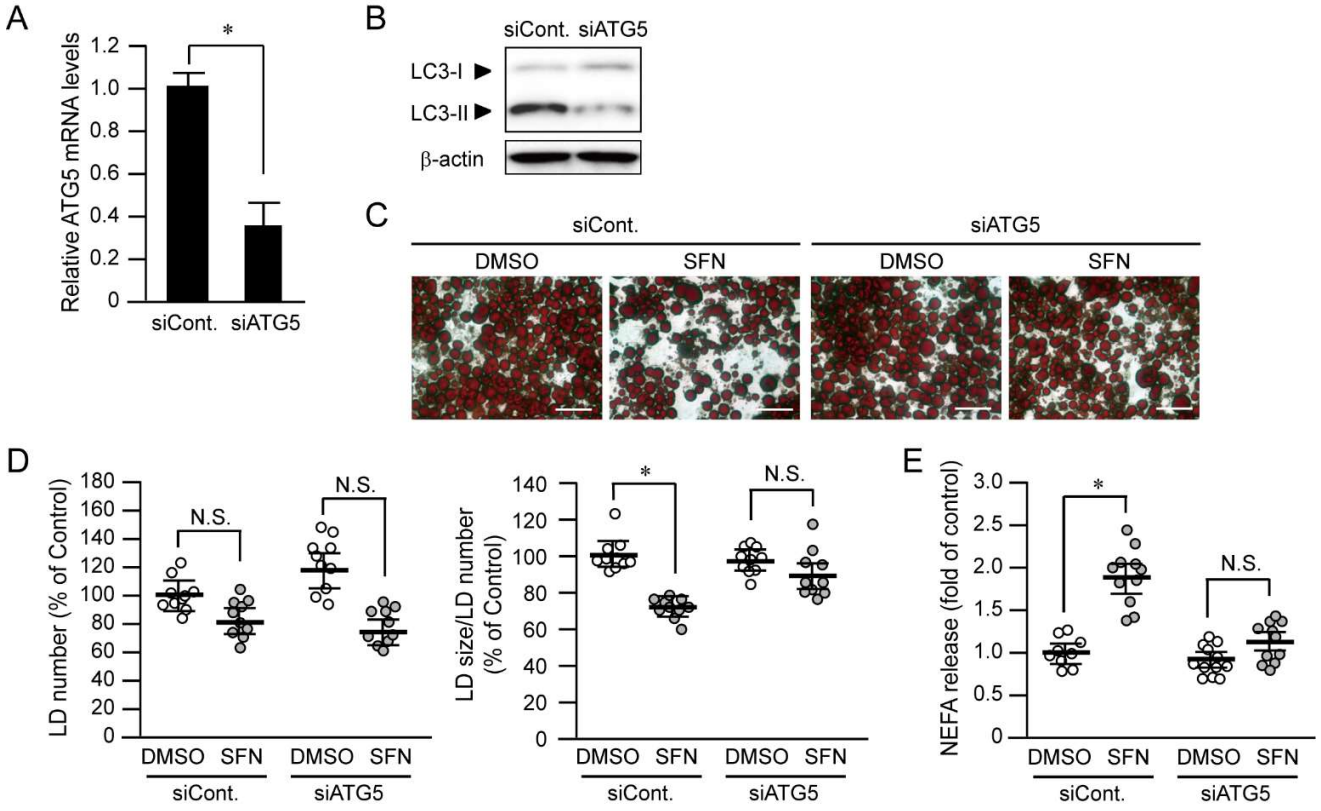

1

2

Figure. 5 Masuda M. et al

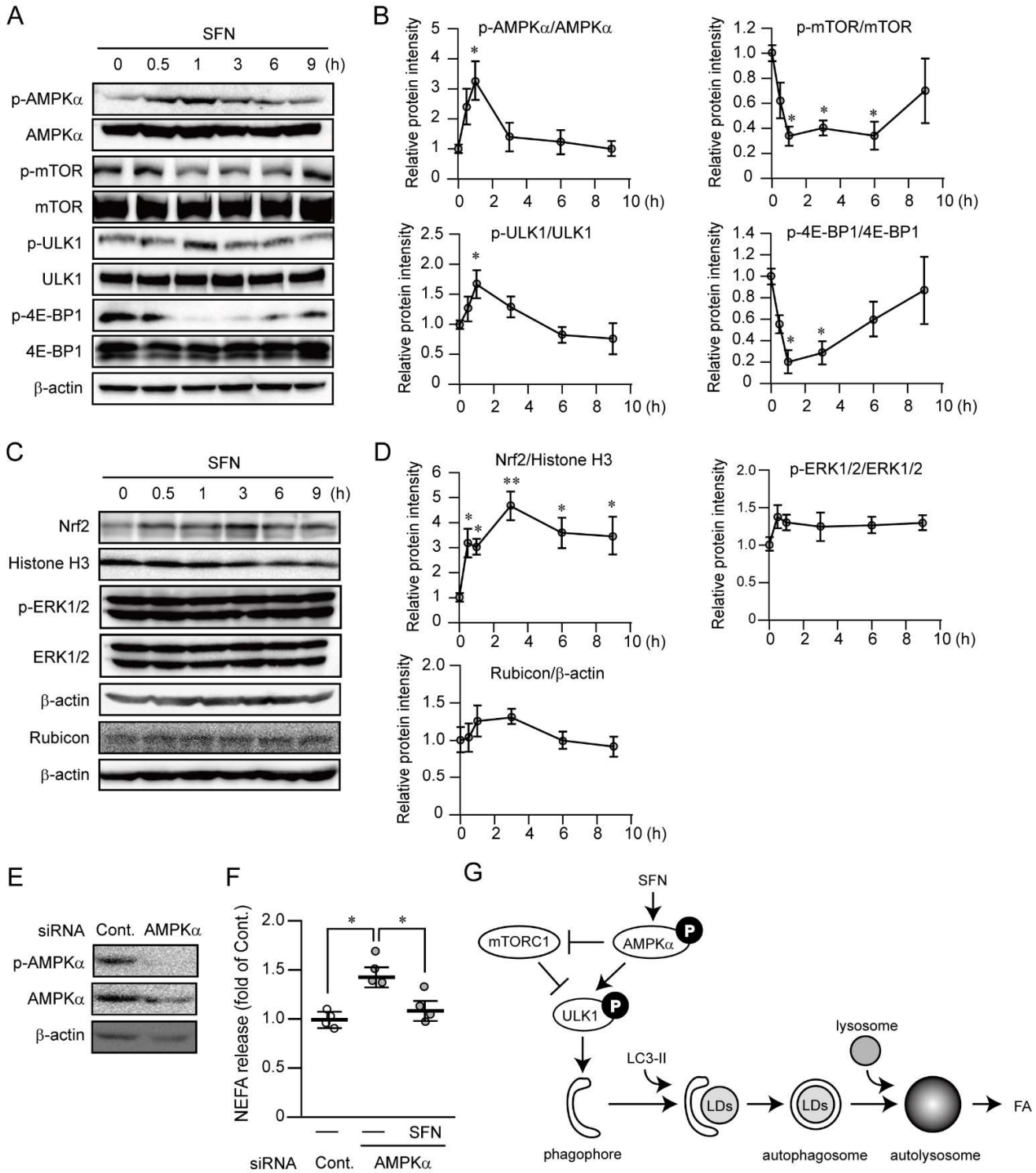

Table 1. Effects of SFN on plasma TG and NEFA levels.

	CFD		HFD	
	DMSO	SFN	DMSO	SFN
TG (mg/dl)	38.1 ± 2.01 [a]	33.0 ± 2.24 [a]	67.5 ± 10.3 [b]	51.3 ± 2.07 [b]
NEFA (mEq/l)	0.431 ± 0.050 [a]	0.436 ± 0.046 [a]	0.584 ± 0.046 [b]	0.507 ± 0.021 [b]

Values are means ± S.E.M. (n = 4). Data was analyzed by a one-way ANOVA with a Student-Newman post-hoc test. Different letters denote significantly distinct groups at $p < 0.05$.

Supplemental Figure. 1 Masuda M. et al

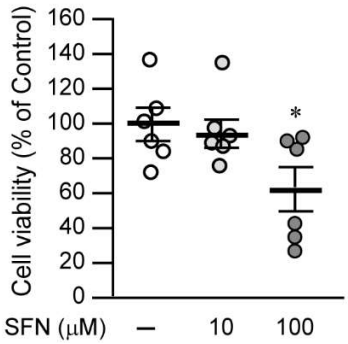

Supplemental Figure. 2 Masuda M. et al

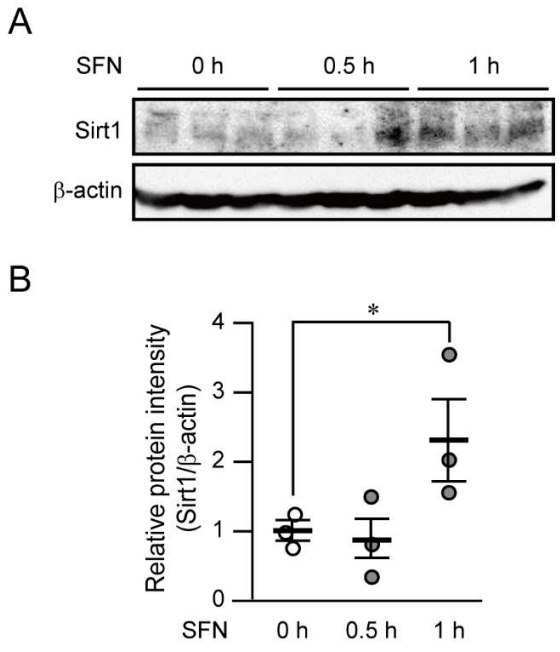

1